

Analysis of axisymmetric boundary layers

Praveen Kumar¹ and Krishnan Mahesh^{1†}

¹Department of Aerospace Engineering and Mechanics, University of Minnesota, Minneapolis, MN 55455, USA

(Received xx; revised xx; accepted xx)

Axisymmetric boundary layers are studied using integral analysis of the governing equations for axial flow over a circular cylinder. The analysis includes the effect of pressure gradient and focuses on the effect of transverse curvature on boundary layer parameters such as shape factor (H) and skin-friction coefficient (C_f), defined as $H = \delta^*/\theta$ and $C_f = \tau_w/(0.5\rho U_e^2)$ respectively, where δ^* is displacement thickness, θ is momentum thickness, τ_w is the shear stress at the wall, ρ is density and U_e is the streamwise velocity at the edge of the boundary layer. Relations are obtained relating the mean wall-normal velocity at the edge of the boundary layer (V_e) and C_f to the boundary layer and pressure gradient parameters. The analytical relations reduce to established results for planar boundary layers in the limit of infinite radius of curvature. The relations are used to obtain C_f which shows good agreement with the data reported in the literature. The analytical results are used to discuss different flow regimes of axisymmetric boundary layers in the presence of pressure gradients.

1. Introduction

Turbulent boundary layers (TBL) are one of the most studied canonical fluid problems but most past studies are devoted to the flat plate (planar) TBL. A recent review by Smits *et al.* (2011) describes the current understanding and future challenges of wall-bounded flows at high Reynolds number (Re). A variety of hydrodynamic engineering applications however, involve axisymmetric TBL, which involve an additional length scale parameter to account for curvature. Several engineering applications have axisymmetric TBL evolving under the influence of pressure gradients due to their geometrical shapes. For example, figure 1 shows a generic submarine hull (Groves *et al.* 1989) along with the streamwise varying pressure gradients experienced by the hull boundary layer.

The radius based Reynolds number ($Re_a = aU/\nu$, where U is freestream velocity, ν is kinematic viscosity and a is the radius of cylinder) does not include any effect of wall-shear stress or boundary layer thickness. Therefore, popular non-dimensional parameters to characterize axisymmetric TBL are the ratio of boundary layer thickness to the radius of curvature (δ/a) and the radius of curvature in wall units (a^+). Based on these two parameters, three regimes can be identified (Piquet & Patel 1999): (i) both δ/a and a^+ are large, (ii) large δ/a and small a^+ and (iii) small δ/a and large a^+ . The first flow regime is observed for axial flow over a long slender cylinder at high Re , where large effect of curvature is felt. The second flow regime is realized for axial flow over slender cylinders at low Re , where axisymmetric TBL behaves like an axisymmetric wake with an inner layer with strong curvature and low-Re effects. Almost all the experimental studies reported in the literature have focused on the first two regimes (see Piquet & Patel 1999). The third flow regime is common in applications where the Reynolds number is high but the boundary layer is thin compared to the radius of curvature. Usually, this flow regime

† Email address for correspondence: kmahesh@umn.edu

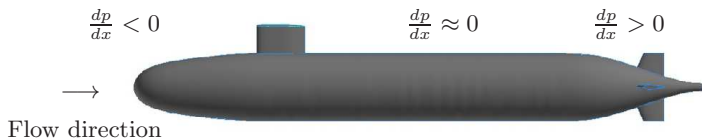


FIGURE 1. Different pressure gradient conditions experienced by the streamwise (x) evolving hull boundary layer on a generic submarine hull, AFF8 (Groves *et al.* 1989).

is treated as a planar boundary layer where the curvature effects are assumed minimal. Although, there are significant fundamental differences between a planar TBL and a thin axisymmetric TBL at high Re , such as increased skin-friction and rapid radial decay in turbulence away from the wall (Lueptow 1990).

One of the earliest analytical investigation of the effect of transverse curvature on skin-friction was conducted by Landweber (1949), who used a $1/7^{th}$ -power-law for velocity profile and the Blasius skin-friction law (Schlichting 1968) to show that for a given momentum thickness (θ) based Reynolds number (Re_θ), axisymmetric boundary layers have higher skin-friction and lower boundary layer thickness in comparison to planar boundary layers. Seban & Bond (1951) analysed the laminar boundary layer for axial flow over a circular cylinder from the governing boundary layer equations and showed that the skin-friction and heat-transfer coefficients for axisymmetric laminar boundary layers are higher than that obtained from the Blasius solution. Kelly (1954) introduced an important correction to their solution, known as the Seban-Bond-Kelly (SBK) solution for zero pressure gradient (ZPG) axisymmetric boundary layers. The SBK solution was extended to the regime of large curvature effect as encountered in axial flow over long thin cylinders by Glauert & Lighthill (1955). Stewartson (1955) provided an asymptotic solution for ZPG laminar axial flow over long thin cylinders.

Axisymmetric TBL have not received the same attention as planar TBL likely due to the inherent difficulties in keeping the flow perfectly axial and prevent sagging or elastic deformation of the cylinders. The effect of curvature has been the focus of most past studies. Richmond (1957) and Yu (1958) conducted the first few experimental studies for curvature effects on boundary layers, which was followed by extensive experimental studies (Rao 1967; Cebeci 1970; Rao & Keshavan 1972; Chase 1972; Patel 1974; Patel *et al.* 1974; Willmarth *et al.* 1976; Luxton *et al.* 1984; Lueptow *et al.* 1985; Krane *et al.* 2010) showing that the transverse curvature indeed has a significant effect on the overall behaviour of axisymmetric TBL.

Afzal & Narasimha (1976) analysed thin axisymmetric TBL at high Re (regime 3 described above) using asymptotic expansions and modified the well-known classical law of the wall for planar TBL to include the effect of curvature. The wall-normal distance in wall units (y^+) was modified as,

$$y^+ = a^+ \ln(1 + y/a) \quad (1.1)$$

where, $a^+ = au_\tau/\nu$ is the radius of curvature in wall-units. Using this modified y^+ , it was shown that there exists a log layer in the mean velocity profile similar to that found in planar TBL, with same slope but the intercept (B) is a weak function of curvature ($B = 5 + 236/a^+$). It has been shown that $U^+ = a^+ \ln(1 + y/a)$ is valid in the viscous sublayer region, but the use of y^+ from eq. 1.1 instead of the planar y^+ in the logarithmic

region assumes that transverse curvature affects both the viscous sublayer and log layer identically.

One of the earliest numerical simulations of axisymmetric boundary layers were performed by Cebeci (1970), who showed higher skin-friction compared to flat plate prediction in both laminar and turbulent regimes. Similar behaviour of skin-friction was observed in numerous subsequent simulations of axisymmetric TBL. Axisymmetric TBL over long thin cylinders have been extensively studied by Tutty (2008) using Reynolds-averaged Navier–Stokes (RANS) and Jordan (2011, 2013, 2014*a,b*) using direct numerical simulations (DNS) and large eddy simulations (LES). Jordan used his simulation database to propose simple models for the skin-friction (Jordan 2013) and the flow field (Jordan 2014*b*).

None of the studies mentioned so far have considered pressure gradient effects. Experiments by Fernholz & Warnack (1998) and Warnack & Fernholz (1998) considered axisymmetric TBL under favourable pressure gradient (FPG) in internal flow.

Boundary layers under adverse pressure gradients (APG) have been studied in the past using asymptotic expansions (See Afzal 1983, 2008) and references therein). Recently, Wei & Klewicki (2016) performed integral analysis of the governing equations for ZPG boundary layers over flat plates and obtained,

$$\frac{U_e V_e}{u_\tau^2} = H \quad (1.2)$$

where U_e and V_e are the mean streamwise and wall-normal velocity at the edge of the boundary layer respectively, H is the shape factor and $u_\tau = \sqrt{\tau_w/\rho}$ is the friction velocity. The analysis was later extended for planar boundary layers under pressure gradient by Wei *et al.* (2017), which modified eq. 1.2 as,

$$\frac{U_e V_e}{u_\tau^2} = H + (1 + \delta/\delta^* + H)\beta_{RC} \quad (1.3)$$

where β_{RC} is the Rotta–Clauser pressure gradient parameter (Rotta 1953; Clauser 1954), δ^* is the displacement thickness and δ is the boundary layer thickness. β_{RC} is often used to quantify the strength of APG in boundary layer flows.

The goal of the present work is to analyse the governing equations of axisymmetric boundary layers evolving under the influence of pressure gradient and understand the effect of transverse curvature on the flow. Integral analysis of the governing equations is performed in §2 and the obtained relations are compared to the existing data in §3. Implications of analytical relations are discussed in §4. §5 concludes the paper.

2. Integral analysis of axisymmetric boundary layer

The boundary layer approximations for the time-averaged Navier–Stokes equations in cylindrical coordinates yield,

$$r \frac{\partial U}{\partial x} + \frac{\partial(rV)}{\partial r} = 0, \quad (2.1)$$

$$rU \frac{\partial U}{\partial x} + rV \frac{\partial U}{\partial r} = -\frac{r}{\rho} \frac{dP}{dx} + \frac{\partial(r\nu \frac{\partial U}{\partial r})}{\partial r} + \frac{\partial(-r\overline{u'v'})}{\partial r} \quad (2.2)$$

where U and V are mean, and u' and v' are fluctuations in axial and radial velocities respectively. Note that the stress term involving $\partial(\overline{u'u'} - \overline{v'v'})/\partial x$ has been ignored on the right hand side of eq. 2.2 for the present analysis. This term however, can not be neglected for large magnitude of pressure gradients and boundary layers on the verge of

separation. We have not made any assumption on the nature of boundary layer i.e. it can be laminar, transitional or turbulent. This implies that the present analysis holds as long as the governing equations (eqs. 2.1, 2.2) are valid.

For boundary layer under pressure gradient, the mean wall-normal velocity outside the boundary layer (V_o) is not constant. Hence, the boundary layer equations are integrated in wall-normal direction from the surface, $r = a$ to a location outside the boundary layer, $r = a + k\delta$ where a is the radius of curvature (cylinder), $k \geq 1$ is a parameter and δ is the boundary layer thickness. Note that setting $k = 1$ makes $V_o = V_e$, which is the mean wall-normal velocity at the edge of the boundary layer. Integration of eqs. 2.1 and 2.2 with the aforementioned limits yield,

$$\begin{aligned} \int_a^{a+k\delta} r \frac{\partial U}{\partial x} dr &= - \int_a^{a+k\delta} \frac{\partial(rV)}{\partial r} dr = - \left(rV \right) \Big|_a^{a+k\delta} \\ &= -(a+k\delta)V_o, \end{aligned} \quad (2.3)$$

$$\begin{aligned} \int_a^{a+k\delta} rU \frac{\partial U}{\partial x} dr + \int_a^{a+k\delta} rV \frac{\partial U}{\partial r} dr &= - \int_a^{a+k\delta} \frac{r}{\rho} \frac{dp}{dx} dr + \int_a^{a+k\delta} \frac{\partial(r\nu \frac{\partial U}{\partial r})}{\partial r} dr + \int_a^{a+k\delta} \frac{\partial(-r\overline{u'v'})}{\partial r} dr \\ &= -\beta_{RC} \frac{u_\tau^2}{2\delta^*} r^2 \Big|_a^{a+k\delta} + \left(r\nu \frac{\partial U}{\partial r} \right) \Big|_a^{a+k\delta} - (r\overline{u'v'}) \Big|_a^{a+k\delta} \end{aligned} \quad (2.4)$$

where β_{RC} is defined as,

$$\beta_{RC} = \frac{\delta^*}{u_\tau^2} \frac{1}{\rho} \frac{dP}{dx} = -\frac{\delta^*}{u_\tau^2} U_e \frac{dU_e}{dx} \quad (2.5)$$

and $f \Big|_a^b = f(b) - f(a)$. Using the boundary conditions,

$$U \Big|_a = 0, \quad U \Big|_{a+k\delta} = U_e, \quad (2.6)$$

$$V \Big|_a = 0, \quad V \Big|_{a+k\delta} = V_o, \quad (2.7)$$

$$\frac{\partial U}{\partial r} \Big|_a = u_\tau^2/\nu, \quad \frac{\partial U}{\partial r} \Big|_{a+k\delta} = 0, \quad (2.8)$$

$$(-\overline{u'v'}) \Big|_a = (-\overline{u'v'}) \Big|_{a+k\delta} = 0, \quad (2.9)$$

the right hand side of eq. 2.4 can be evaluated. This yields,

$$\begin{aligned} &\int_a^{a+k\delta} rU \frac{\partial U}{\partial x} dr + \int_a^{a+k\delta} rV \frac{\partial U}{\partial r} dr = -\beta_{RC} \frac{u_\tau^2}{2\delta^*} r^2 \Big|_a^{a+k\delta} - au_\tau^2 \\ \implies &\int_a^{a+k\delta} rU \frac{\partial U}{\partial x} dr + (rVU) \Big|_a^{a+k\delta} - \int_a^{a+k\delta} U \frac{\partial(rV)}{\partial r} dr = -\beta_{RC} \frac{u_\tau^2}{2\delta^*} r^2 \Big|_a^{a+k\delta} - au_\tau^2 \\ \implies &\int_a^{a+k\delta} rU \frac{\partial U}{\partial x} dr + (a+k\delta)V_oU_e + \int_a^{a+k\delta} rU \frac{\partial U}{\partial x} dr = -\beta_{RC} \frac{u_\tau^2}{2\delta^*} r^2 \Big|_a^{a+k\delta} - au_\tau^2 \\ \implies &\int_a^{a+k\delta} r \frac{\partial U^2}{\partial x} dr = -(a+k\delta)V_oU_e - \beta_{RC} \frac{u_\tau^2}{2\delta^*} r^2 \Big|_a^{a+k\delta} - au_\tau^2. \end{aligned} \quad (2.10)$$

The shape factor, H is defined as,

$$H = \frac{\delta^*}{\theta}. \quad (2.11)$$

Differentiating both sides with respect to x ,

$$\frac{dH}{dx} = \frac{1}{\theta} \frac{d\delta^*}{dx} - \frac{\delta^*}{\theta^2} \frac{d\theta}{dx} \quad (2.12)$$

$$\implies \theta \frac{dH}{dx} = \frac{d\delta^*}{dx} - H \frac{d\theta}{dx} \quad (2.13)$$

$$\implies H = \frac{\frac{d\delta^*}{dx}}{\frac{d\theta}{dx}} - \theta \frac{\frac{dH}{dx}}{\frac{d\theta}{dx}}. \quad (2.14)$$

Note that no assumption has been made regarding the self-similarity of the boundary layer as yet. The second term in the right hand side of eq. 2.14 is small as H varies very slowly with x as compared to δ^* and hence, can be neglected. Self-similarity implies $\frac{dH}{dx} = 0$, which makes the second term identically zero. Therefore,

$$H = \left(\frac{d\delta^*}{dx} \right) / \left(\frac{d\theta}{dx} \right). \quad (2.15)$$

δ^* and θ for axisymmetric boundary layers are defined (Luxton *et al.* 1984) such that,

$$(\delta^* + a)^2 - a^2 = 2 \int_a^{a+\delta} \left(1 - \frac{U}{U_e} \right) r dr, \quad (2.16)$$

$$(\theta + a)^2 - a^2 = 2 \int_a^{a+\delta} \frac{U}{U_e} \left(1 - \frac{U}{U_e} \right) r dr. \quad (2.17)$$

Note that $U = U_e$ for $r \geq \delta$, hence eqs. 2.16 and 2.17 can be written as,

$$(\delta^* + a)^2 - a^2 = 2 \int_a^{a+k\delta} \left(1 - \frac{U}{U_e} \right) r dr, \quad (2.18)$$

$$(\theta + a)^2 - a^2 = 2 \int_a^{a+k\delta} \frac{U}{U_e} \left(1 - \frac{U}{U_e} \right) r dr, \quad (2.19)$$

since $k \geq 1$.

Differentiating both sides with respect to x and using the Leibniz integral rule in the right hand side yield,

$$2(\delta^* + a) \frac{d\delta^*}{dx} = -\frac{2}{U_e} \int_a^{a+k\delta} \frac{\partial(rU)}{\partial x} dr + \frac{2}{U_e} \frac{dU_e}{dx} I \quad (2.20)$$

$$\begin{aligned} 2(\theta + a) \frac{d\theta}{dx} &= \frac{2}{U_e} \int_a^{a+k\delta} \frac{\partial(rU)}{\partial x} dr - \frac{2}{U_e} \frac{dU_e}{dx} I \\ &\quad - \frac{2}{U_e^2} \int_a^{a+k\delta} \frac{\partial(rU^2)}{\partial x} dr + \frac{4}{U_e} \frac{dU_e}{dx} J \end{aligned} \quad (2.21)$$

where,

$$I = \int_a^{a+k\delta} \frac{U}{U_e} r dr, \quad (2.22)$$

$$J = \int_a^{a+k\delta} \frac{U^2}{U_e^2} r dr. \quad (2.23)$$

Using eqs. 2.3 and 2.10 in the right hand side of eqs. 2.20 and 2.21 yield,

$$2(\delta^* + a) \frac{d\delta^*}{dx} = 2 \frac{V_o}{U_e} (a + k\delta) - 2 \frac{\beta_{RC}}{\delta^*} \frac{u_\tau^2}{U_e^2} I, \quad (2.24)$$

$$\begin{aligned} 2(\theta + a) \frac{d\theta}{dx} &= -2 \frac{V_o}{U_e} (a + k\delta) + 2 \frac{\beta_{RC}}{\delta^*} \frac{u_\tau^2}{U_e^2} I \\ &+ 2 \frac{V_o}{U_e} (a + k\delta) + \frac{\beta_{RC}}{\delta^*} \frac{u_\tau^2}{U_e^2} r^2 \Big|_a^{a+k\delta} + 2a \frac{u_\tau^2}{U_e^2} - 4 \frac{\beta_{RC}}{\delta^*} \frac{u_\tau^2}{U_e^2} J \\ \implies 2(\theta + a) \frac{d\theta}{dx} &= 2a \frac{u_\tau^2}{U_e^2} + 2 \frac{\beta_{RC}}{\delta^*} \frac{u_\tau^2}{U_e^2} I + \frac{\beta_{RC}}{\delta^*} \frac{u_\tau^2}{U_e^2} r^2 \Big|_a^{a+k\delta} - 4 \frac{\beta_{RC}}{\delta^*} \frac{u_\tau^2}{U_e^2} J. \end{aligned} \quad (2.25)$$

Dividing eq. 2.24 by eq. 2.25 and using eq. 2.15 followed by rearranging the terms, we get,

$$\left(\frac{\delta^* + a}{\theta + a} \right) H = \left[\frac{2 \frac{V_o}{U_e} (a + k\delta) - 2 \frac{\beta_{RC}}{\delta^*} \frac{u_\tau^2}{U_e^2} I}{2a \frac{u_\tau^2}{U_e^2} + 2 \frac{\beta_{RC}}{\delta^*} \frac{u_\tau^2}{U_e^2} I + \frac{\beta_{RC}}{\delta^*} \frac{u_\tau^2}{U_e^2} r^2 \Big|_a^{a+k\delta} - 4 \frac{\beta_{RC}}{\delta^*} \frac{u_\tau^2}{U_e^2} J} \right]. \quad (2.26)$$

Using the definitions of δ^* (eq. 2.18) and θ (eq. 2.19), it can be shown that,

$$I = \frac{r^2}{2} \Big|_a^{a+k\delta} - \frac{r^2}{2} \Big|_a^{a+\delta^*}, \quad (2.27)$$

$$J = \frac{r^2}{2} \Big|_a^{a+k\delta} - \frac{r^2}{2} \Big|_a^{a+\delta^*} - \frac{r^2}{2} \Big|_a^{a+\theta}. \quad (2.28)$$

Also, eq. 2.24 yields,

$$\begin{aligned} (\delta^* + a) \frac{d\delta^*}{dx} &= \frac{V_o}{U_e} (a + k\delta) - \frac{\beta_{RC}}{\delta^*} \frac{u_\tau^2}{U_e^2} I \\ \implies \frac{V_o}{U_e} (a + k\delta) &= (\delta^* + a) \frac{d\delta^*}{dx} + \frac{\beta_{RC}}{2\delta^*} \frac{u_\tau^2}{U_e^2} \left(r^2 \Big|_a^{a+k\delta} - r^2 \Big|_a^{a+\delta^*} \right). \end{aligned} \quad (2.29)$$

Hence, eq. 2.26 can be rearranged to show that,

$$\begin{aligned} \left(\frac{\delta^* + a}{\theta + a} \right) H &\left[2a \frac{u_\tau^2}{U_e^2} + \frac{\beta_{RC}}{\delta^*} \frac{u_\tau^2}{U_e^2} \left(r^2 \Big|_a^{a+k\delta} - r^2 \Big|_a^{a+\delta^*} \right) + \frac{\beta_{RC}}{\delta^*} \frac{u_\tau^2}{U_e^2} r^2 \Big|_a^{a+k\delta} \right. \\ &\quad \left. - 2 \frac{\beta_{RC}}{\delta^*} \frac{u_\tau^2}{U_e^2} \left(r^2 \Big|_a^{a+k\delta} - r^2 \Big|_a^{a+\delta^*} - r^2 \Big|_a^{a+\theta} \right) \right] = \quad (2.30) \\ &2 \frac{V_o}{U_e} (a + k\delta) - \frac{\beta_{RC}}{\delta^*} \frac{u_\tau^2}{U_e^2} \left(r^2 \Big|_a^{a+k\delta} - r^2 \Big|_a^{a+\delta^*} \right) \\ \implies 2 \frac{V_o U_e}{u_\tau^2} (a + k\delta) \left(\frac{\theta + a}{\delta^* + a} \right) &= H \left[2a + \frac{\beta_{RC}}{\delta^*} \left(r^2 \Big|_a^{a+\delta^*} + 2r^2 \Big|_a^{a+\theta} \right) \right] \\ &+ \left(\frac{\theta + a}{\delta^* + a} \right) \frac{\beta_{RC}}{\delta^*} \left(r^2 \Big|_a^{a+k\delta} - r^2 \Big|_a^{a+\delta^*} \right). \end{aligned} \quad (2.31)$$

Substituting for V_o from eq. 2.29 and rearranging,

$$\begin{aligned}
 (\theta + a) \frac{d\delta^*}{dx} &= H \frac{u_\tau^2}{U_e^2} \left[a + \frac{\beta_{RC}}{2\delta^*} \left(r^2 \Big|_a^{a+\delta^*} + 2r^2 \Big|_a^{a+\theta} \right) \right] \\
 \implies \frac{u_\tau^2}{U_e^2} &= \frac{(\theta + a) \frac{d\delta^*}{dx}}{H \left[a + \frac{\beta_{RC}}{2\delta^*} \left(r^2 \Big|_a^{a+\delta^*} + 2r^2 \Big|_a^{a+\theta} \right) \right]} \\
 \implies C_f &= \frac{2(1 + \frac{\theta}{a}) \frac{d\delta^*}{dx}}{H + \beta_{RC} \left[2 + H \left(1 + \frac{\delta^*}{2a} + \frac{\theta^2}{a\delta^*} \right) \right]}. \tag{2.32}
 \end{aligned}$$

Self-similarity of boundary layers implies that δ^*/δ is constant. So C_f can be written as,

$$C_f = \frac{2(1 + \frac{\theta}{a}) \frac{\delta^*}{\delta} \frac{d\delta}{dx}}{H + \beta_{RC} \left[2 + H \left(1 + \frac{\delta^*}{2a} + \frac{\theta^2}{a\delta^*} \right) \right]}. \tag{2.33}$$

Note that $C_f = 2u_\tau^2/U_e^2$ is related to β_{RC} by definition (see eq. 2.5). But that definition contains external flow parameters. On the other hand, eq. 2.33 relates C_f to the boundary layer parameters directly. Also, eq. 2.31 can be rearranged to show that,

$$\begin{aligned}
 \frac{U_e V_o}{u_\tau^2} \left(\frac{1 + \theta/a}{1 + \delta^*/a} \right) \left(1 + k \frac{\delta}{a} \right) &= \\
 H + \beta_{RC} \left[2 + H \left(1 + \frac{\delta^*}{2a} + \frac{\theta^2}{a\delta^*} \right) + \left(\frac{1 + \theta/a}{1 + \delta^*/a} \right) \left(k \frac{\delta}{\delta^*} - 1 + \frac{k^2 \delta^2 - \delta^{*2}}{2a\delta^*} \right) \right] & \tag{2.34}
 \end{aligned}$$

At the edge of the boundary layer, $k = 1$ and $V_o = V_e$. Therefore,

$$\begin{aligned}
 \frac{U_e V_e}{u_\tau^2} \left(\frac{1 + \theta/a}{1 + \delta^*/a} \right) \left(1 + \frac{\delta}{a} \right) &= \\
 H + \beta_{RC} \left[2 + H \left(1 + \frac{\delta^*}{2a} + \frac{\theta^2}{a\delta^*} \right) + \left(\frac{1 + \theta/a}{1 + \delta^*/a} \right) \left(\frac{\delta}{\delta^*} - 1 + \frac{\delta^2 - \delta^{*2}}{2a\delta^*} \right) \right]. & \tag{2.35}
 \end{aligned}$$

At the verge of separation, u_τ goes to zero. Using the definition of β_{RC} (eq. 2.5), eq. 2.35 yields,

$$\begin{aligned}
 V_e = -\delta^* \frac{dU_e}{dx} \left(\frac{1 + \theta/a}{1 + \delta^*/a} \right)^{-1} \left(1 + \frac{\delta}{a} \right)^{-1} & \left[2 + H \left(1 + \frac{\delta^*}{2a} + \frac{\theta^2}{a\delta^*} \right) \right. \\
 & \left. + \left(\frac{1 + \theta/a}{1 + \delta^*/a} \right) \left(\frac{\delta}{\delta^*} - 1 + \frac{\delta^2 - \delta^{*2}}{2a\delta^*} \right) \right]. \tag{2.36}
 \end{aligned}$$

3. Comparison to previous work

3.1. Consistency with planar boundary layers relations

For a planar boundary layer, $1/a$ approaches 0 as a approaches ∞ . Setting $1/a = 0$ in eq. 2.33 and 2.34 yields,

$$C_f = \frac{2\frac{\delta^*}{\delta}\frac{d\delta}{dx}}{H + \beta_{RC}(2 + H)}, \quad \text{and} \quad (3.1)$$

$$\frac{U_e V_o}{u_\tau^2} = H + \beta_{RC} \left(1 + H + k \frac{\delta}{\delta^*} \right). \quad (3.2)$$

At the verge of separation, $u_\tau = 0$; setting $k = 1$ yields,

$$V_e = -\delta^* \frac{dU_e}{dx} \left(1 + H + \frac{\delta}{\delta^*} \right). \quad (3.3)$$

These relations are identical to those derived by Wei *et al.* (2017) (eq. 13 and 14 of their paper) for planar boundary layer with pressure gradient. They compared their analytical relations to the data available in literature for APG TBL and found good agreement (see figure 2-5 of their paper).

Setting $\beta_{RC} = 0$ in eq. 3.2 yields,

$$\frac{U_e V_o}{u_\tau^2} = H. \quad (3.4)$$

Note that for $\beta_{RC} = 0$, regardless of the value of k , V_o is same i.e. $V_o = V_e$ is constant outside the boundary layer. Eq. 3.4 was derived by Wei & Klewicki (2016) (eq. 11 of their paper) and shown to be valid for laminar, transitional and turbulent boundary layers.

3.2. Axisymmetric ZPG laminar boundary layer

The SBK solution (Seban & Bond 1951; Kelly 1954) for axisymmetric laminar boundary layer is valid up to $\frac{\nu x}{U a^2} < 0.04$, and was subsequently extended by Glauert & Lighthill (1955) to the interval $0.04 < \frac{\nu x}{U a^2} < 100$. For ZPG laminar axisymmetric boundary layer, eq. 2.33 becomes,

$$C_{f,axisymmetric} = 2 \frac{d\theta}{dx} \left(1 + \frac{\theta}{a} \right) = C_{f,planar} \left(1 + \frac{\delta^*}{aH} \right). \quad (3.5)$$

δ^* can be obtained from either SBK or GL solutions and $H = 2.59$ for a laminar boundary layer. Thus, C_f can be obtained. Figure 2(a) shows C_f as a function of $\frac{\nu x}{U a^2}$ for three different $Re_a = 10000, 1000$ and 500 , compared with both SBK and GL solutions. Note that the difference in C_f using δ^* from either solution (SBK or GL) is negligible. Our results smoothly transitions from SBK to GL solution as $\frac{\nu x}{U a^2}$ increases, as evident in the lower Re_a cases. Figure 2(b) compares our result with the numerical solution of Cebeci (1970), where Re_a is varied. δ^* and H for this case are estimated from the asymptotic results of Stewartson (1955). The C_f obtained from the Blasius solution ($C_f \sqrt{Re_x} = 0.664$) (Schlichting 1968) is also shown for comparison. Overall, our results show good agreement with Cebeci (1970) for the entire range from thin to thick axisymmetric laminar boundary layer. Note that at large Re_a , δ/a approaches zero and hence, the axisymmetric laminar boundary layer approaches planar behaviour.

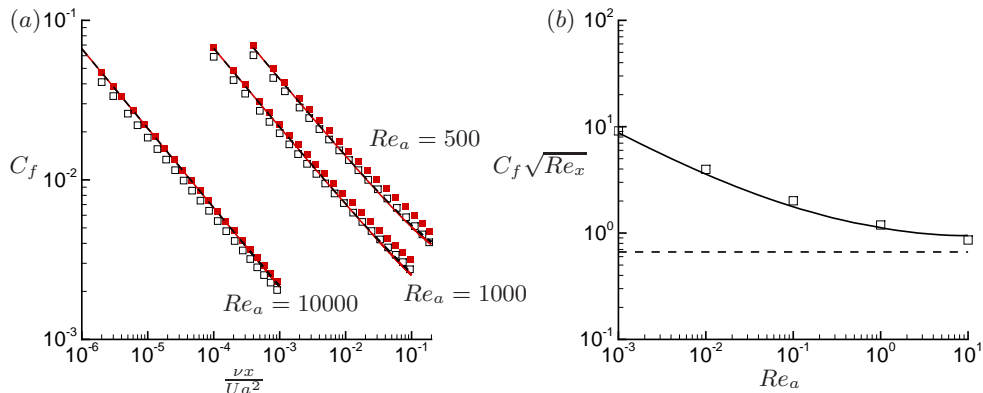


FIGURE 2. Skin-friction coefficient (C_f) as a function of non-dimensional parameter $\frac{\nu x}{Ua^2}$ (a), where results for radius based Reynolds number $Re_a = 500, 1000$ and 10000 are shown along with solutions of Seban-Bond-Kelly (Seban & Bond 1951; Kelly 1954) (■) and Glauert-Lighthill (Glauert & Lighthill 1955) (□). The present result (eq. 3.5) using δ^* from SBK (—) and GL (---), show identical C_f . C_f as a function of Re_a is compared with the result of Cebeci (1970) (□) for long thin cylinder (large x/a), where boundary layer thickness reaches asymptotic value (Stewartson 1955)(b). The value obtained from the Blasius solution (---) is also shown in (b) for comparison.

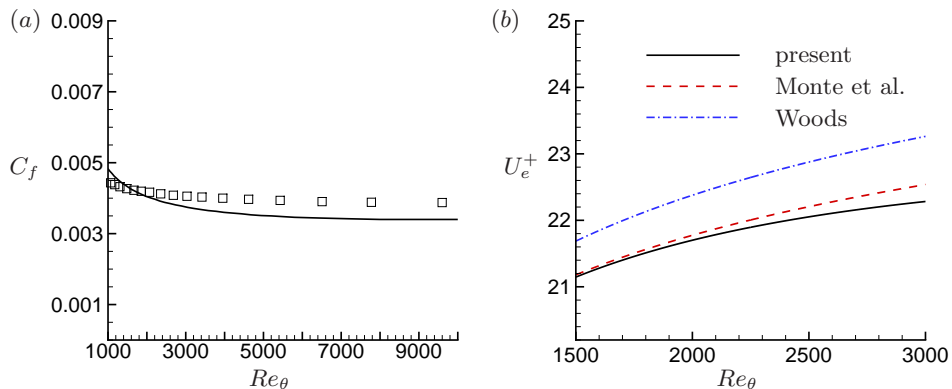


FIGURE 3. (a) Skin-friction coefficient (C_f) as a function of Re_θ is compared with the result of Cebeci (1970) (□) for slender cylinder for radius based Reynolds number $Re_a = 40200$ and radius $a = 1''$. The shape factor of $H = 1.4$ and $C_{f,planar}$ correlation of Monkewitz *et al.* (2008) is used in our relation to predict C_f . The boundary layer growth is assumed identical to that of flat plate, which need not be true for slender cylinders at high Re_θ . (b) U_e^+ as a function of Re_θ is compared with the correlations of Monte *et al.* (2011) and Woods (2006). U_e^+ is related to C_f as $U_e^+ = \sqrt{2/C_f}$.

3.3. Axisymmetric ZPG turbulent boundary layer

Cebeci (1970) numerically solved incompressible turbulent ZPG axial flow over a circular slender cylinder of radius, $a = 1''$ and $Re_a = 40200$. The same relation eq. 3.5 is used to estimate C_f but the $C_{f,planar}$ correlation of Monkewitz *et al.* (2008) is used. The shape factor H is assumed to be 1.4 and the boundary layer growth $d\theta/dx$ is assumed identical in both planar and axisymmetric case. Figure 3 (a) shows our results compared to that of Cebeci (1970). Note that the range of Re_θ on the cylinder is large

($1000 < Re_\theta < 10000$). Hence, the assumption of identical growth and $H = 1.4$ may not hold, which is the reason for the difference between our result and that of Cebeci (1970). In reality, H is a weakly decreasing function of Re_θ for TBL (Monkewitz *et al.* 2008). For example, $H \approx 1.45$ at $Re_\theta = 1000$ (Schlatter & Örlü 2010), whereas $H \approx 1.36$ at $Re_\theta = 9000$ (Österlund 1999). The results shown in figure 3 (a) will further improve if the variation of H with Re_θ is taken into account.

Kumar & Mahesh (2016) simulated thin axisymmetric TBL in the range $1400 < Re_\theta < 1620$. Using their boundary layer δ^* and θ variation with streamwise distance x , which is almost linear, their slope $d\delta^*/dx$ and $d\theta/dx$ can be estimated. This estimated slope can be used to compute C_f for $1500 < Re_\theta < 3000$ as shown in figure 3(b). Our results are compared with correlation of Monte *et al.* (2011), which corrected the correlation of Woods (2006) using their extensive simulation database, showing good agreement. Note that for a large range of Re_θ , the assumption of linear growth of boundary layer breaks down, hence the differences at large Re_θ .

4. Discussion

4.1. Effect of curvature on C_f

If both planar and axisymmetric boundary layers have the same boundary layer parameters, eqs. 2.33 and 3.1 yield:

$$\begin{aligned} \frac{C_{f,axisymmetric}}{C_{f,planar}} &= \frac{\left(1 + \frac{\theta}{a}\right) \left[H + \beta_{RC} (2 + H) \right]}{H + \beta_{RC} \left[2 + H \left(1 + \frac{\delta^*}{2a} + \frac{\theta^2}{a\delta^*} \right) \right]} \\ \implies \frac{C_{f,axisymmetric}}{C_{f,planar}} - 1 &= \frac{\frac{\theta}{a} H + \beta_{RC} \left[\frac{\theta}{a} + \frac{\delta^*}{a} \left(1 - \frac{H}{2} \right) \right]}{H + \beta_{RC} \left[2 + H \left(1 + \frac{\delta^*}{2a} + \frac{\theta^2}{a\delta^*} \right) \right]}. \end{aligned} \quad (4.1)$$

Thus, if the right hand side of eq. 4.1 is positive, the presence of curvature increases C_f and vice-versa.

It is easy to see that for ZPG ($\beta_{RC} = 0$) boundary layers,

$$\frac{C_{f,axisymmetric}}{C_{f,planar}} = 1 + \frac{\theta}{a}. \quad (4.2)$$

For boundary layer with APG ($\beta_{RC} > 0$), the denominator of the right hand side of eq. 4.1 is always positive. Hence, the effect of curvature will depend on the sign of the numerator η defined as,

$$\eta = \frac{\theta}{a} H + \beta_{RC} \left[\frac{\theta}{a} + \frac{\delta^*}{a} \left(1 - \frac{H}{2} \right) \right]. \quad (4.3)$$

It can be shown that $\eta \geq 0$ if $\beta_{RC} \geq 0$ (see appendix A). Therefore, the presence of curvature increases C_f if $\beta_{RC} \geq 0$. Note that, this is true regardless of the value of a . It has been assumed that $d\delta/dx$ is identical for both planar and axisymmetric TBL. This is not be always true. In fact, for thick axisymmetric TBL at zero-pressure-gradient ($\delta/a \gg 1$ and $\beta_{RC} = 0$), $d\delta/dx$ is smaller than that of planar TBL value (Tutty 2008). However, C_f is still higher than planar values because $\theta/a \gg 1$, which compensates for the decrease in $d\delta/dx$.

The presence of curvature may or may not increase C_f in FPG axisymmetric TBL depending on the sign of the right hand side of eq. 4.1.

4.2. Thick axisymmetric ZPG turbulent boundary layer

For $\beta_{RC} = 0$, the expression for C_f (eq. 2.33) reduces to,

$$C_f = 2 \left(1 + \frac{\theta}{a} \right) \frac{\theta}{\delta} \frac{d\delta}{dx}. \quad (4.4)$$

Thus, knowing local boundary layer parameters, C_f can be estimated. For example, Jordan (2014a) compiled numerous experimental results along with his simulation database for thick axisymmetric TBL in ZPG and showed that $\delta/\theta \approx 7.2$. The estimated value of $d\delta/dx \approx 2.5 \times 10^{-3}$ for a range of thick axisymmetric TBL ($2.1 \leq \delta/a \leq 11$, $37 \leq a^+ \leq 388$, $586 \leq Re_a \leq 7475$). This makes,

$$C_f = 6.94 \times 10^{-4} \left(1 + \frac{\theta}{a} \right) = 6.94 \times 10^{-4} \left(1 + \frac{Re_\theta}{Re_a} \right). \quad (4.5)$$

4.3. Axisymmetric turbulent boundary layer under large APG

For large APG, $\beta_{RC} \gg 1$. Thus eq. 2.33 yields,

$$C_f \approx \left[\frac{2(1 + \frac{\theta}{a}) \frac{\delta^*}{\delta} \frac{d\delta}{dx}}{2 + H \left(1 + \frac{\delta^*}{2a} + \frac{\theta^2}{a\delta^*} \right)} \right] \frac{1}{\beta_{RC}}. \quad (4.6)$$

For self-similar TBL in APG, δ^*/δ , H and $d\delta/dx$ become constant (Maciel *et al.* 2006). Similar behaviour is expected for axisymmetric TBL as well. When $\delta/a < 1$, θ/a and δ^*/a are small as compared to 1. This makes, the term inside brackets ([]) nearly constant. Thus for thin axisymmetric TBL at large APG, $C_f \sim 1/\beta_{RC}$. A similar result was obtained by Wei *et al.* (2017) for planar TBL.

4.4. Axisymmetric turbulent boundary layer under FPG

For FPG TBL, there are two important flow parameters: pressure gradient parameter (Λ) (Narasimha & Sreenivasan 1973) and acceleration parameter (K) (Launder 1964) defined as,

$$\Lambda = -\frac{\delta}{u_\tau^2} \frac{1}{\rho} \frac{dP}{dx}, \quad (4.7)$$

$$K = \frac{\nu}{U_e^2} \frac{dU_e}{dx}. \quad (4.8)$$

All the relations derived in §2 holds for FPG axisymmetric TBL as well by replacing β_{RC} with $-\Lambda$. It can be shown that,

$$\frac{dC_f}{d\Lambda} = C_f \left[\frac{2 + H \left(1 + \frac{\delta^*}{a} + \frac{\theta^2}{a\delta^*} \right)}{H - \Lambda \left[2 + H \left(1 + \frac{\delta^*}{a} + \frac{\theta^2}{a\delta^*} \right) \right]} \right] < 0. \quad (4.9)$$

Thus, increasing FPG decreases C_f and this effect is expected to be enhanced by the presence of transverse curvature as the presence of terms with $1/a$ enhance the magnitude of $dC_f/d\Lambda$.

5. Conclusion

In this work, the integral analysis of equations governing axisymmetric boundary layer flow is presented, including the effect of pressure gradient. Analytical relations are derived relating C_f to the boundary layer parameters. The relations for planar TBL with and without pressure gradient presented by Wei *et al.* (2017) and Wei & Klewicki (2016) respectively can be recovered by setting $1/a = 0$ and further setting $\beta_{RC} = 0$. It has been shown that the presence of transverse curvature increases C_f regardless of the nature of boundary layer, consistent with the observations reported in the literature for both ZPG and APG axisymmetric boundary layers. The derived relations are compared to the existing results in the literature showing good agreement. The results presented in this work are expected to be valid for any boundary layer as long as the governing equations hold, which assumes local dynamic equilibrium. It is challenging, both experimentally and computationally, to obtain accurate C_f at high Re . However, it is relatively easier to obtain accurate mean velocity profiles. In addition to predicting the influence of pressure gradient and curvature, the derived expressions are potentially useful to both skin-friction measurements and wall-modelled large eddy simulation of turbulent boundary layers.

Acknowledgement

This work is supported by the United States Office of Naval Research (ONR) under ONR Grant N00014-14-1-0289 with Dr. Ki-Han Kim as technical monitor. We thank Mr. S. Anantharamu for useful discussions.

Appendix A. Maximum value of η

It is known that, $H \geq 1$ which yields,

$$\frac{H}{2} \geq \frac{1}{2} \implies \frac{H}{2} - 1 \geq -\frac{1}{2}, \quad (\text{A } 1)$$

$$\frac{1}{H} \leq 1 \implies -\frac{1}{H} \geq -1. \quad (\text{A } 2)$$

Adding eqs. A 1 and A 2 we get,

$$\frac{H}{2} - 1 - \frac{1}{H} \geq -\frac{3}{2}, \implies \frac{1}{\frac{H}{2} - 1 - \frac{1}{H}} \leq -\frac{2}{3}. \quad (\text{A } 3)$$

But,

$$\frac{1}{\frac{H}{2} - 1 - \frac{1}{H}} = \frac{H}{H(\frac{H}{2} - 1) - 1} = \frac{-\frac{\theta}{a}H}{\frac{\theta}{a} + H\frac{\theta}{a}\left(1 - \frac{H}{2}\right)} = \frac{-\frac{\theta}{a}H}{\frac{\theta}{a} + \frac{\delta^*}{a}\left(1 - \frac{H}{2}\right)}. \quad (\text{A } 4)$$

From eqs. A 3 and A 4, it follows that,

$$\frac{-\frac{\theta}{a}H}{\frac{\theta}{a} + \frac{\delta^*}{a}\left(1 - \frac{H}{2}\right)} \leq -\frac{2}{3}. \quad (\text{A } 5)$$

Now,

$$\eta = \frac{\theta}{a}H + \beta_{RC} \left[\frac{\theta}{a} + \frac{\delta^*}{a} \left(1 - \frac{H}{2} \right) \right] > 0$$

$$\iff \beta_{RC} > \frac{-\frac{\theta}{a}H}{\frac{\theta}{a} + \frac{\delta^*}{a} \left(1 - \frac{H}{2} \right)}. \quad (\text{A } 6)$$

Using eq. A 5, it is easy to see that eq. A 6 always holds for $\beta_{RC} > 0$.

REFERENCES

- AFZAL, N. 1983 Analysis of a turbulent boundary layer subjected to a strong adverse pressure gradient. *International Journal of Engineering Science* **21** (6), 563–576.
- AFZAL, N. 2008 Turbulent boundary layer with negligible wall stress. *Journal of Fluids Engineering* **130** (5), 051205.
- AFZAL, N. & NARASIMHA, R. 1976 Axisymmetric turbulent boundary layer along a circular cylinder at constant pressure. *Journal of Fluid Mechanics* **74** (1), 113–128.
- CEBECI, T. 1970 Laminar and turbulent incompressible boundary layers on slender bodies of revolution in axial flow. *Journal of Basic Engineering* **92**, 545–554.
- CHASE, D. M. 1972 Mean velocity profile of a thick turbulent boundary layer along a circular cylinder. *AIAA Journal* **10** (7), 849–850.
- CLAUSER, F. H. 1954 Turbulent boundary layers in adverse pressure gradients. *J. Aeronaut. Sci* **21** (2), 91–108.
- FERNHOLZ, H. H. & WARNACK, D. 1998 The effects of a favourable pressure gradient and of the Reynolds number on an incompressible axisymmetric turbulent boundary layer. part 1. the turbulent boundary layer. *Journal of Fluid Mechanics* **359**, 329–356.
- GLAUERT, M. B. & LIGHTHILL, M. J. 1955 The axisymmetric boundary layer on a long thin cylinder. In *Proceedings of the Royal Society of London A: Mathematical, Physical and Engineering Sciences*, , vol. 230, pp. 188–203. The Royal Society.
- GROVES, NANCY C, HUANG, THOMAS T & CHANG, MING S 1989 *Geometric Characteristics of DARPA Suboff Models:(DTRC Model Nos. 5470 and 5471)*. David Taylor Research Center.
- JORDAN, S. A. 2011 Axisymmetric turbulent statistics of long slender circular cylinders. *Physics of Fluids (1994-present)* **23** (7), 075105.
- JORDAN, S. A. 2013 A skin friction model for axisymmetric turbulent boundary layers along long thin circular cylinders. *Physics of Fluids (1994-present)* **25** (7), 075104.
- JORDAN, S. A. 2014a On the axisymmetric turbulent boundary layer growth along long thin circular cylinders. *Journal of Fluids Engineering* **136** (5), 051202.
- JORDAN, S. A. 2014b A simple model of axisymmetric turbulent boundary layers along long thin circular cylinders. *Physics of Fluids (1994-present)* **26** (8), 085110.
- KELLY, H. R. 1954 A note on the laminar boundary layer on a circular cylinder in axial incompressible flow. *Journal of the Aeronautical Sciences* .
- KRANE, M. H., GREGA, L. M. & WEI, T. 2010 Measurements in the near-wall region of a boundary layer over a wall with large transverse curvature. *Journal of Fluid Mechanics* **664**, 33–50.
- KUMAR, P. & MAHESH, K. 2016 Towards large eddy simulation of hull-attached propeller in crashback. In *Proceedings of the 31st Symposium on Naval Hydrodynamics, Monterey, USA*.
- LANDWEBER, L. 1949 Effect of transverse curvature on frictional resistance. *Tech. Rep.*. David Taylor Model Basin Washington DC.
- LAUNDER, BE 1964 Laminarization of the turbulent boundary layer in a severe acceleration. *Journal of Applied Mechanics* **31** (4), 707–708.
- LUEPTOW, R. M. 1990 Turbulent boundary layer on a cylinder in axial flow. *AIAA Journal* **28** (10), 1705–1706.
- LUEPTOW, R. M., LEEHEY, P. & STELLINGER, T. 1985 The thick, turbulent boundary layer

- on a cylinder: Mean and fluctuating velocities. *Physics of Fluids (1958-1988)* **28** (12), 3495–3505.
- LUXTON, R. E., BULL, M. K. & RAJAGOPALAN, S. 1984 The thick turbulent boundary layer on a long fine cylinder in axial flow. *Aeronautical Journal* **88**, 186–199.
- MACIEL, Y., ROSSIGNOL, K.-S. & LEMAY, J. 2006 Self-similarity in the outer region of adverse-pressure-gradient turbulent boundary layers. *AIAA journal* **44** (11), 2450–2464.
- MONKEWITZ, P. A., CHAUHAN, K. A. & NAGIB, H. M. 2008 Comparison of mean flow similarity laws in zero pressure gradient turbulent boundary layers. *Physics of Fluids (1994-present)* **20** (10), 105102.
- MONTE, S., SAGAUT, P. & GOMEZ, T. 2011 Analysis of turbulent skin friction generated in flow along a cylinder. *Physics of Fluids (1994-present)* **23** (6), 065106.
- NARASIMHA, R. & SREENIVASAN, K. R. 1973 Relaminarization in highly accelerated turbulent boundary layers. *Journal of Fluid Mechanics* **61** (3), 417–447.
- ÖSTERLUND, J. M. 1999 Experimental studies of zero pressure-gradient turbulent boundary layer flow. PhD thesis, Royal Institute of Technology, Stockholm, Sweden.
- PATEL, V. C. 1974 A simple integral method for the calculation of thick axisymmetric turbulent boundary layers. *The Aeronautical Quarterly* **25** (1), 47–58.
- PATEL, V. C., NAKAYAMA, A. & DAMIAN, R. 1974 Measurements in the thick axisymmetric turbulent boundary layer near the tail of a body of revolution. *Journal of Fluid Mechanics* **63** (2), 345–367.
- PIQUET, J. & PATEL, V. C. 1999 Transverse curvature effects in turbulent boundary layer. *Progress in Aerospace Sciences* **35** (7), 661–672.
- RAO, G. N. V. 1967 The law of the wall in a thick axisymmetric turbulent boundary layer. *ASME J. Appl. Mech* **89**, 237–338.
- RAO, G. N. V. & KESHAVAN, N. R. 1972 Axisymmetric turbulent boundary layers in zero pressure-gradient flows. *Journal of Applied Mechanics* **39** (1), 25–32.
- RICHMOND, R. L. 1957 Experimental investigation of thick, axially symmetric boundary layers on cylinders at subsonic and hypersonic speeds. PhD thesis, California Institute of Technology.
- ROTTA, J. 1953 On the theory of the turbulent boundary layer. *NACA Technical Memorandum, No. 1344*.
- SCHLATTER, P. & ÖRLÜ, R. 2010 Assessment of direct numerical simulation data of turbulent boundary layers. *Journal of Fluid Mechanics* **659**, 116–126.
- SCHLICHTING, H. 1968 Boundary-layer theory.
- SEBAN, R. A. & BOND, R. 1951 Skin-friction and heat-transfer characteristics of a laminar boundary layer on a cylinder in axial incompressible flow. *Journal of the Aeronautical Sciences* **18** (10), 671–675.
- SMITS, A. J., MCKEON, B. J. & MARUSIC, I. 2011 High-Reynolds number wall turbulence. *Annual Review of Fluid Mechanics* **43**, 353–375.
- STEWARTSON, K. 1955 The asymptotic boundary layer on a circular cylinder in axial incompressible flow. *Quarterly of Applied Mathematics* **13** (2), 113–122.
- TUTTY, O. R. 2008 Flow along a long thin cylinder. *Journal of Fluid Mechanics* **602**, 1–37.
- WARNACK, D. & FERNHOLZ, H. H. 1998 The effects of a favourable pressure gradient and of the Reynolds number on an incompressible axisymmetric turbulent boundary layer. part 2. the boundary layer with relaminarization. *Journal of Fluid Mechanics* **359**, 357–381.
- WEI, T. & KLEWICKI, J. 2016 Scaling properties of the mean wall-normal velocity in zero-pressure-gradient boundary layers. *Physical Review Fluids* **1** (8), 082401.
- WEI, T., MACIEL, Y. & KLEWICKI, J. 2017 Integral analysis of boundary layer flows with pressure gradient. *Physical Review Fluids* **2** (9), 092601.
- WILLMARTH, W. W., WINKEL, R. E., SHARMA, L. K. & BOGAR, T. J. 1976 Axially symmetric turbulent boundary layers on cylinders: Mean velocity profiles and wall pressure fluctuations. *Journal of Fluid Mechanics* **76** (01), 35–64.
- WOODS, M. J. 2006 *Computation of axial and near-axial flow over a long circular cylinder*. University of Adelaide, Australia.
- YU, Y. S. 1958 Effects of transverse curvature on turbulent boundary layer characteristics. *Journal of Ship Research* **3**, 33–41.